Journal of Biomedical Optics

BiomedicalOptics.SPIEDigitalLibrary.org

Holographic fluorescence microscopy with incoherent digital holographic adaptive optics

Changwon Jang
Jonghyun Kim
David C. Clark
Seungjae Lee
Byoungho Lee
Myung K. Kim

SPIE.

Journal of Biomedical Optics 20(11), 111204 (November 2015)

Holographic fluorescence microscopy with incoherent digital holographic adaptive optics

Changwon Jang,[a] Jonghyun Kim,[a] David C. Clark,[b] Seungjae Lee,[a] Byoungho Lee,[a] and Myung K. Kim[b,*]
[a]Seoul National University, School of Electrical Engineering, Gwanak-Gu Gwanakro 1, Seoul 151-744, Republic of Korea
[b]University of South Florida, Department of Physics, ISAA6218, 4202 East Fowler Avenue, Tampa, Florida 33620, United States

Abstract. Introduction of adaptive optics technology into astronomy and ophthalmology has made great contributions in these fields, allowing one to recover images blurred by atmospheric turbulence or aberrations of the eye. Similar adaptive optics improvement in microscopic imaging is also of interest to researchers using various techniques. Current technology of adaptive optics typically contains three key elements: a wavefront sensor, wavefront corrector, and controller. These hardware elements tend to be bulky, expensive, and limited in resolution, involving, for example, lenslet arrays for sensing or multiactuator deformable mirrors for correcting. We have previously introduced an alternate approach based on unique capabilities of digital holography, namely direct access to the phase profile of an optical field and the ability to numerically manipulate the phase profile. We have also demonstrated that direct access and compensation of the phase profile are possible not only with conventional coherent digital holography, but also with a new type of digital holography using incoherent light: selfinterference incoherent digital holography (SIDH). The SIDH generates a complex—i.e., amplitude plus phase—hologram from one or several interferograms acquired with incoherent light, such as LEDs, lamps, sunlight, or fluorescence. The complex point spread function can be measured using guide star illumination and it allows deterministic deconvolution of the full-field image. We present experimental demonstration of aberration compensation in holographic fluorescence microscopy using SIDH. Adaptive optics by SIDH provides new tools for improved cellular fluorescence microscopy through intact tissue layers or other types of aberrant media. [DOI: 10.1117/1.JBO.20.11.111204]

Keywords: adaptive optics; digital holography; self-interference; incoherent digital holography; fluorescence microscopy.
Paper 150169SSPR received Mar. 16, 2015; accepted for publication Jun. 8, 2015; published online Jul. 6, 2015.

1 Introduction

1.1 *Self-Interference Incoherent Digital Holography*

In conventional digital holography, the interference between the object and reference beams is recorded as a hologram using coherent illumination. The information of the object is encoded in the interference pattern. Numerical propagation of the generated complex hologram to a desired plane provides a reconstructed image of the object based on diffraction theory.[1] Access to the complex information of optical fields allows for useful image processing techniques;[2,3] however, the need for coherent light limits the versatility of conventional digital holography. Therefore, efforts have been made to overcome this limitation by acquiring holograms with incoherent light.[4–7] Self-interference incoherent digital holography (SIDH) is one method of generating holograms from spatially incoherent light sources such as LED light or even natural sunlight.[8] Although conventional digital holography requires a separate reference beam in order to achieve interference with an object beam, in SIDH, the signal wavefront from the object is split, then reunited with differential curvature to generate interference. Since the light source is spatially incoherent, the interference pattern of each point source acts as a point spread function and is superposed to generate the hologram. Incoherent digital holography has a remarkable advantage of versatility compared to conventional holography since incoherent light can be utilized to acquire the hologram of the object. In this paper, we focus on fluorescence microscopy as an application of SIDH.

1.2 *Holographic Fluorescence Microscopy with Incoherent Digital Holographic Adaptive Optics*

Fluorescence microscopy is a remarkable technique which can be utilized in various applications such as super-resolution imaging or functional imaging.[9,10] However, since fluorescence is incoherent by nature, digital holography is difficult to apply to fluorescence microscopy. There have been some efforts such as combining quantitative phase microscopy and fluorescence microscopy or adopting mechanical scanning; however, usually they require complicated additional systems.[11–13] Incoherent digital holography can overcome these limitations. By using SIDH, complex holograms can be acquired using fluorescence light[14] and adaptive optics can be applied to fluorescence microscopy. The concept of adaptive optics was first developed by Babcock[15] to compensate possible wavefront distortions in astronomy. In conventional adaptive optics, additional hardware is needed such as lens arrays or deformable mirrors.[16] However, a new method of adaptive optics called incoherent digital holographic adaptive optics (IDHAO) has been recently proposed using digital holographic technique.[17,18] In IDHAO, it is possible to replace conventional hardware with holographic image processing by acquiring complex field information.

*Address all correspondence to: Myung K. Kim, E-mail: mkkim@usf.edu

1083-3668/2015/$25.00

Adaptive optics techniques are used in the astronomy field because turbulence of air causes aberration of the wavefront from a star. Likewise, there is a possibility of aberration when light from a microscopic object propagates through aberrant media such as a tissue layer (or culture medium). By applying adaptive optics in fluorescence microscopy, it is possible to acquire complex holograms of fluorescence microscopic objects through aberrant media.[19] Holographic fluorescence microscopy (HFM) with IDHAO provides new capabilities for fluorescence microscopy and digital holography.

2 Theory

2.1 *Principle of IDHAO*

In an IDHAO system, the object is considered as a set of spatially incoherent point sources which generate separate spherical waves. Each spherical wave interferes with itself after propagating through a modified Michelson interferometer. The intensity of each interference pattern is superposed at the sensor plane. Figure 1 shows the basic IDHAO configuration with an aberration layer.

The corresponding coordinate planes are represented by x_o, x', x_m, and x_c, with the y component omitted for simplicity. The point source is placed at x_o with intensity $I_o = |E_o|^2$. The wave propagates through the aberration layer $\Psi'(x')$ and arrives at the interferometer system, consisting of a beam splitter and two mirrors of different curvatures to produce an interference pattern at CCD plane x_c. If we calculate the optical field at the CCD plane based on Fresnel propagation theory, the wavefront from a point light source which has the optical path reflected by mirror A has field component of

$$\begin{aligned} E_A(x_c) &= \int \mathrm{d}x' \int \mathrm{d}x_m E_o Q_{z''}(x' - x_o)\Psi'(x') \\ &\quad \times Q_{z'}(x_m - x')Q_{-f_A}(x_m)Q_{z_c}(x_c - x_m) \\ &= E_o Q_{z_o - f_A}(x_A)Q_{z_A + z_c}(x_c - x_A)\Phi_A \psi'(x_c - \alpha_A x_o), \end{aligned} \tag{1}$$

where

$$Q_z(x) \equiv \exp\left[\frac{ik}{2z}(x^2)\right], \tag{2}$$

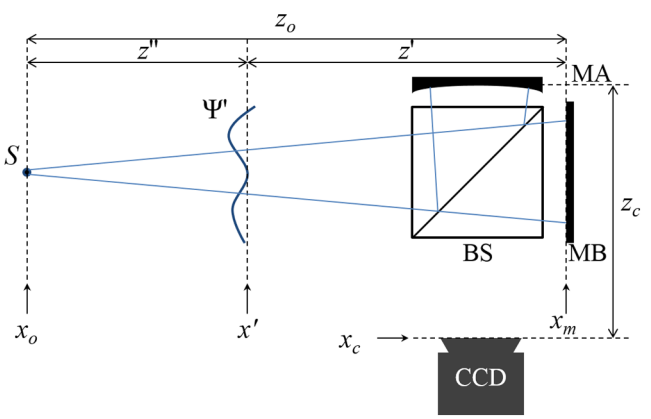

Fig. 1 Basic incoherent digital holographic adaptive optics (IDHAO) configuration: S, point light source; Ψ', aberration layer; BS, beam splitter; MA (MB), concave mirror with focal length f_A and planar mirror.

$$\Phi_A(x) = [\Psi' * Q_{\zeta_A}](\beta_A x) = \int \mathrm{d}x' \Psi'(x') Q_{\zeta_A}(x' - \beta_A x), \tag{3}$$

$$x_A = -\frac{f_A}{z_o - f_A} x_o; \quad z_A = -\frac{f_A}{z_o - f_A} z_o, \tag{4}$$

$$\alpha_A = -\frac{z'}{z''}\frac{z_A + z_c}{z_A} + \alpha, \tag{5}$$

$$\beta_A = \frac{z''}{z'' + z'}\frac{z_A}{z_A + z_c}, \tag{6}$$

$$\zeta_A = \frac{z''}{z'' + z'}\left[z' + \frac{z''}{z'' + z'}\frac{z_A z_c}{z_A + z_c}\right], \tag{7}$$

$$\alpha = -\frac{z_c}{z_o}. \tag{8}$$

The constant complex propagation factor $\exp(ikz)$ is omitted for simplicity and * stands for two-dimensional (2-D) convolution. However, the CCD captures only the intensity of the field component as

$$I_c(x_c) = |E_A + E_B|^2, \tag{9}$$

where E_B is the field component generated by the planar mirror.

The complex hologram can be retrieved with a phase shifting process.[2,3] In this study, three-step phase shifting with a piezoactuator is utilized to capture images with different phases. The acquired complex hologram of a point source has the form of

$$\begin{aligned} &C(x_c; x_o) \\ &\quad = I_o(x_o) Q_{z_{AB}}(x_c - \alpha x_o)\Phi_A(x_c - \alpha_A x_o)\Phi_B^*(x_c - \alpha_B x_o), \end{aligned} \tag{10}$$

where

$$z_{AB} = -\frac{(z_A + z_c)(z_B + z_c)}{z_A - z_B}. \tag{11}$$

If the point source is located at the center of the object plane, the acquired hologram can be interpreted as a complex point spread function (CPSF) of the system or the guide star (GS) hologram which has the form of

$$G_\Psi(x_c) = I_o(x_o) Q_{z_{AB}}(x_c)\Phi_A(x_c)\Phi_B^*(x_c). \tag{12}$$

Since the object is considered as a set of spatially incoherent point sources, integration over all points results in the hologram of the object expressed as

$$\begin{aligned} H_\Psi(x_c) &= \int \mathrm{d}x_o I_o(x_o) Q_{z_{AB}}(x_c - \alpha x_o)\Phi_A(x_c - \alpha_A x_o) \\ &\quad \times \Phi_B(x_c - \alpha_B x_o). \end{aligned} \tag{13}$$

This can be simplified as a convolution form of the magnified object image and the CPSF of system if we set $z' = 0$; then

$$H_\Psi(x_c) = [I_o' * Q_{Z_{AB}}\Phi_A\Phi_B^*](x_c) = [I_o' * G_\Psi](x_c), \tag{14}$$

where

$$I'(x_{co}) = I_o\left(\frac{x_c}{\alpha}\right), \tag{15}$$

$$\alpha = \frac{-z_c}{z_o}. \tag{16}$$

It shows that the object image can be reconstructed, if we have the GS hologram, which is a CPSF $G_\Psi(x_c)$ by calculating the cross-correlation as

$$H_\Psi \otimes G_\Psi = I_o' * [G_\Psi \otimes G_\Psi] = I_o'. \tag{17}$$

2.2 *IDHAO in Microscopy*

A microscopy system has essential optical components such as the objective lens and tube lens. In an infinity-corrected optical imaging system, the objective lens creates an image of an object at infinity, and the tube lens refocuses the image in front of the eye piece. An HFM with an SIDH system can be realized by replacing the eye piece with an interferometer system as shown in Fig. 2.

The object is located at x_{oo} plane with distance of z_{fo} from objective lens, which has focal length of f_o. An aberration layer Ψ_a is located at the plane x_a which is between the objective lens and the object. The tube lens has focal length of f_t and is located at the x_{ft} plane with a distance of z_{ft} from the objective lens. Mirrors MA and MB are each at a distance of z_m from the tube lens and have focal lengths of f_A and f_B, respectively. A CCD camera is located at plane x_c with distance of z_c from the mirrors of interferometer. The optical field at the CCD plane made by the point source which has intensity of I_{oo} at position of (x_{oo}) has the form of

$$\begin{aligned} E(x_c) = \int \mathrm{d}x_m \int \mathrm{d}x_{f_t} \int \mathrm{d}x_{f_o} \int \mathrm{d}x_a E_o Q(x_a - x_{oo})\psi_a(x_a) \\ \times Q_{z_a}(x_{f_o} - x_a) Q_{-f_o}(x_{f_o}) Q_{z_{f_t}}(x_{f_t} - x_{f_o}) \\ \times Q_{-f_t}(x_{f_t}) Q_{z_m}(x_c - x_m) Q_{-f_A}(x_m) Q_{z_c}(x_c - x_m), \end{aligned} \tag{18}$$

$$\begin{aligned} H_\Psi(x_c) = \int dx_{oo} I'_{oo}(x_{oo}) Q_{z_{AB}}(x_c - \alpha_2 x_{oo}) \\ \times \Phi_A(x_c - \alpha_A M_o x_{oo}) \Phi_B^*(x_c - \alpha_B M_o x_{oo}), \end{aligned} \tag{19}$$

where

$$I'(x_{oo}) = I_{oo}\left(\frac{x}{\alpha_2}\right), \tag{20}$$

$$\alpha_2 = \frac{-z_c}{z_o} M_o, \tag{21}$$

where the functions and parameters are defined at the same manner as Sec. 2.1, and

$$\Psi(x) = \Psi_a(M_a x), \tag{22}$$

$$M_o = \frac{x_o}{x_{oo}} = \frac{f_o f_t}{(z_{f_o} - f_o)\left[z_t + \left(\frac{-f_o}{z_{f_o} - f_o}\right) z_{f_o} - f_t\right]}, \tag{23}$$

$$M_a = \frac{x'}{x_a} = \frac{f_o f_t}{(z_a - f_o)\left[z_t + \left(\frac{-f_o}{z_a - f_o}\right) z_a - f_t\right]}, \tag{24}$$

$$z_o = z_m - \frac{-f_t\left(z_{f_t} + \frac{f_o z_{f_o}}{f_o + z_{f_o}}\right)}{f_t - \left(z_{f_t} + \frac{f_o z_{f_o}}{f_o + z_{f_o}}\right)}, \tag{25}$$

$$z' = z_m - \frac{-f_t\left(z_{f_t} + \frac{f_o z_{f_a}}{f_o + z_{f_a}}\right)}{f_t - \left(z_{f_t} + \frac{f_o z_{f_a}}{f_o + z_{f_a}}\right)}, \tag{26}$$

$$z'' = z_o - z' \simeq \frac{-f_t\left(z_{f_t} + \frac{f_o z_{f_a}}{f_o + z_{f_a}}\right)}{f_t - \left(z_{f_t} + \frac{f_o z_{f_a}}{f_o + z_{f_a}}\right)} - f_t. \tag{27}$$

In this case, if we set

$$z_a = \frac{(z_m f_t - z_m z_t + f_t z_t)}{(z_m - f_t) f_o + (z_m f_t - z_m z_t + f_t z_t)} f_o, \tag{28}$$

the case gives the same result as $z' = 0$ in Eq. (7), where the acquired hologram is expressed in convolution form of object image and GS hologram, as follows:

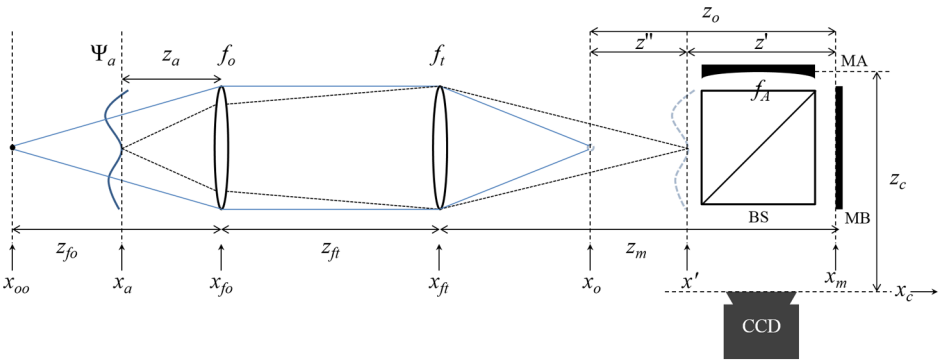

Fig. 2 Configuration of IDHAO in microscopy. Ψ_a, aberration layer; BS, beam splitter; MA (MB), concave mirror with focal length f_A and planar mirror.

$$H_\Psi(x_c) = I'_{oo} * G_\Psi(x_c), \tag{29}$$

where I'_{oo} is the scaled image of I_{oo} magnified by α_2. Equation (29) indicates that the image could be perfectly recovered theoretically, when the aberration layer is located at a certain plane. As will be demonstrated and discussed in this paper, the IDHAO process is robust with respect to the location of aberration layer. Also, we can simply set the aberration layer to z_a in a practical situation by adjusting the location of the object. Since the acquired hologram is expressed in convolution form, the microscopic object image can be reconstructed by calculating the correlation with the GS hologram, which we call the GS reconstruction method, as well as in the microscopy system.

3 Experiment and Results

3.1 *Optical Setup of Holographic Fluorescence Microscopy*

The whole system can be separated into two parts: a microscopy system and an SIDH system. The microscopy system magnifies and images the fluorescent microscopic object through objective and tube lenses. The SIDH system is located after the microscopy system, as depicted in Fig. 3, and consists of a beam splitter and two optical path matched mirrors with different curvatures. In this case, a concave mirror and a planar mirror are used to generate interference of light from the fluorescent object. A USAF 1951 resolution target with fluorescence back plate and diffuser is used as the fluorescent object. The transparent elements of the resolution target generate the fluorescent image. The aberration layer can be modeled as a layer located between the microscopic object and objective lens which has irregular shaped or irregular refractive indexed surface which distorts the wavefront from the microscopic object. Therefore, the object image is distorted at the imaging plane and cannot be observed clearly without correction. In this study, a piece of broken glass which has an irregular-shaped surface is used as an aberration layer. A mercury lamp is used for excitation light source and illuminates the object through a dichroic mirror and excitation filter. We use an Olympus U-FBW filter set as our dichroic mirror and excitation filter which has a 505 nm cutoff frequency and 460 to 495 nm bandwidths, respectively. An emission filter which has a center frequency of 530 nm (10 nm bandwidth) is located after the tube lens. An objective lens and a tube lens magnify and refocus the image to a certain plane. We built an SIDH system which consists of a beam splitter and two mirrors at the end of the microscopy system. The wavefront is duplicated with differential curvature by a concave mirror which has a focal length of 500 mm and a planar mirror, and is united again to generate an interference pattern. Phase shifting is conducted by a piezoactuator which is attached to the backside of the planar mirror. The piezoactuator and CCD camera are controlled by a computer and a three-step phase shifting process is introduced to retrieve the integral of the complex hologram.[2,3] We used a 35-μm pinhole with a diffuser and fluorescence back plate as a GS since 35 μm is small enough to be considered as a point light source in the 7×7 mm^2 field-of-view. The GS generates spherical wave which propagates through the microscopy system and the SIDH system to form a Fresnel zone plate interference pattern at the CCD plane as described in Sec. 2. With the phase shifting process, the complex hologram of the GS can be acquired which represents the CPSF of the HFM with IDHAO system. In the practical situation of cellular imaging, we expect the GS can be incorporated in several ways, such as an injected fluorescent bead or a fluorescent-labeled organelle, or a high-powered focused light which can act as a point source.

3.2 *Result: Conventional Reconstruction versus IDHAO Reconstruction*

Numerical reconstruction of the image is conducted using the acquired complex holograms. MATLAB (Mathworks 2014b) is used as a simulation tool and parula colormap is used which has consistency between intensity and brightness. In the presence of an aberration layer, the wavefront is distorted and the acquired hologram produces a distorted image reconstruction. Therefore, a GS hologram is captured to measure and compensate the distortion caused by the aberration layer. Figure 4 shows the amplitude and phase image of the distorted complex holograms of the object and GS. Without an aberration layer, the phase image of the GS hologram is expected to form a Fresnel zone pattern which converges and forms a delta function when propagated through free space. However, in this aberrated case, there is distortion of the phase image of the GS hologram as shown in Fig. 4(d). Therefore, when the wavefront propagates, the energy does not converge to a single point but forms an arbitrary pattern through the propagation distances along the z-axis. If we consider the effect of wavefront distortion in a hologram, propagation will not result in an in-focus reconstruction but instead a

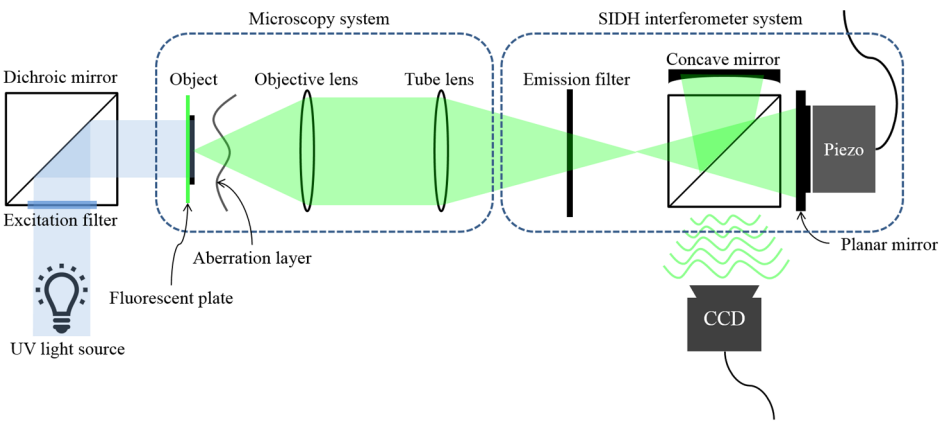

Fig. 3 Configuration of experimental setup for holographic fluorescence microscopy with IDHAO system.

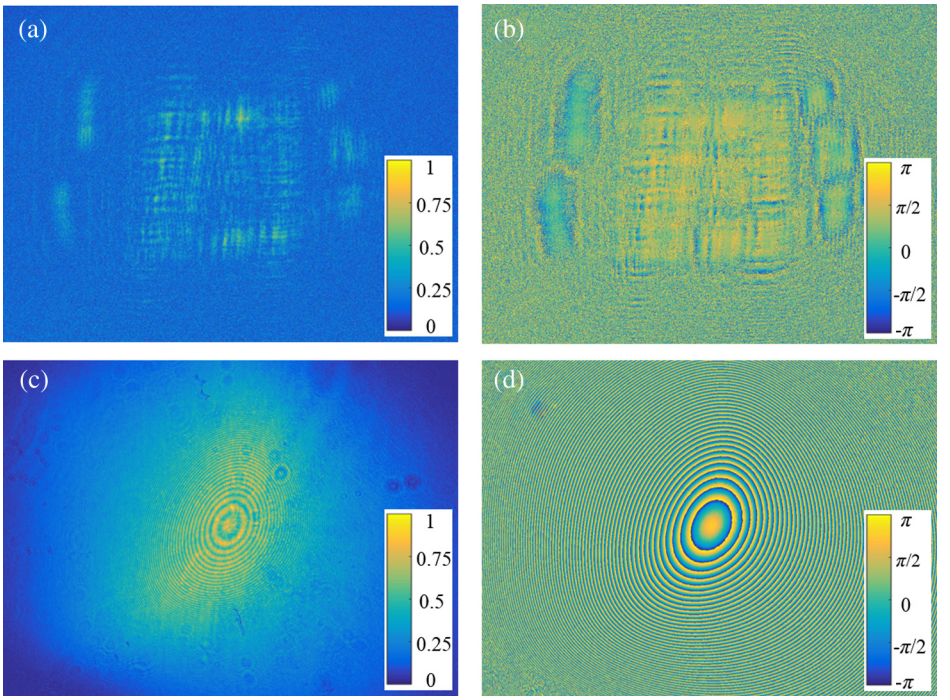

Fig. 4 Acquired holograms of the object and the guide star (GS): (a) amplitude of the object hologram (in a normalized arbitrary unit), (b) phase of the object hologram ($-\pi$ to π), (c) amplitude of the GS hologram, and (d) phase of the GS hologram.

blurred and distorted image. Figure 5(a) shows amplitude images of the propagated wavefront of the magnified GS hologram and the target hologram at propagation distances near the expected focus plane. Angular spectrum method diffraction is used for the numerical propagation. No obvious best-focused image is obtained due to the distortions and blurring effects. In order to decide the best focusing propagation distance, the maximum intensity value of the image of the GS hologram is measured by varying the propagation distance and the result is shown in Fig. 5(b). From this result, the case of III in Fig. 5(a) could be decided as a best reconstructed image from numerical propagation and is shown in Fig. 6(a). We then performed image reconstruction by calculating the 2-D cross-correlation of the object hologram and GS hologram as described in Sec. 2.2. Figure 6(b) shows the image reconstructed by the GS reconstruction method, which is the main result of this study. In Fig. 6(a), we can see that the image suffers from low contrast and severe distortion caused by the aberration. On the other hand, Fig. 6(b) shows remarkably enhanced image quality in contrast with the case of Fig. 6(a). This shows that the CPSF contains the information of the phase aberration and can be used to restore the original signal from a distorted wavefront.

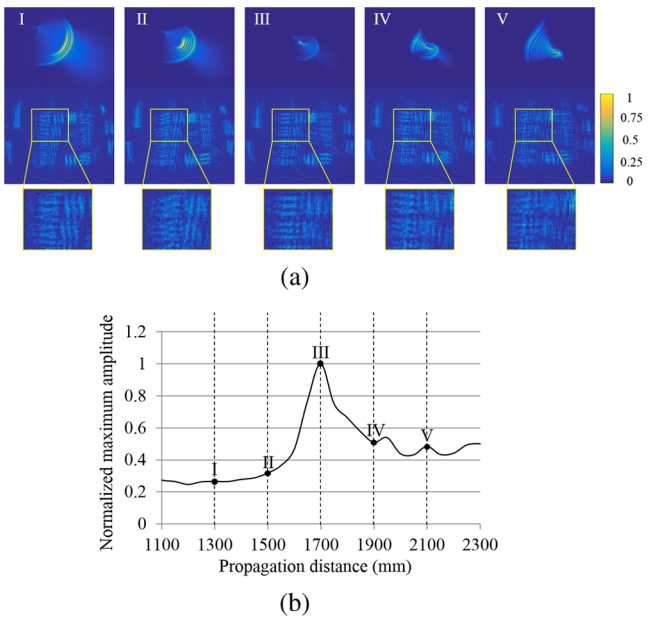

Fig. 5 (a) Numerically reconstructed focused images of GS hologram varying the propagation distance near the estimated focusing distance and (b) a graph of maximum intensity value of focused images.

3.3 *Result 2: AO Reconstruction with a Moving Position of the Aberration Layer*

As described in Sec. 2, there is a theoretical desired location of aberration layer, dependent on the system parameters, to compensate the image perfectly by the GS reconstruction method. This is because in that position, the acquired complex hologram of the object has the form of exact convolution between GS hologram and the object image. However, even if the aberration layer is not located exactly at the desired position or has a certain thickness, the GS reconstruction still shows better results compared to the numerical propagation reconstruction. To show the feasibility, we designed an experiment of the GS reconstruction (HFM with IDHAO) varying the position of aberration layer z_a. Basically, the apparatus is the same as Sec. 3.2, but we additionally installed a motorized linear stage for the aberrator which has a position resolution of 1 μm in order to move the aberration layer position. The holograms of the object and GS are acquired

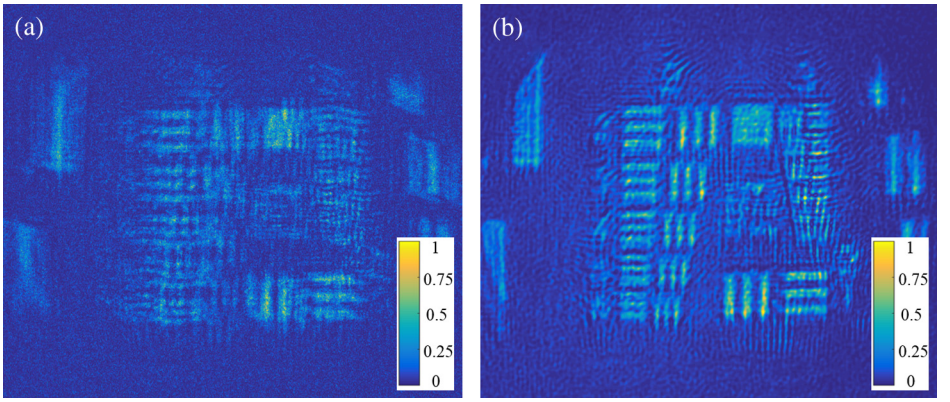

Fig. 6 Best focused images of numerically reconstructed result using: (a) conventional propagation method and (b) GS reconstruction method.

in the same manner as in Sec. 3.1 while varying the position of the aberration layer.

Figures 7(a)–7(d) show the amplitude and phase images of the acquired object hologram and GS hologram, respectively, when the aberration layer is located at the theoretically desired location. Figure 7(e) shows the shape of the amplitude image distortion for the aberrator used in this experiment when numerically propagated through the expected focus range. The best reconstruction distance is decided by comparing the maximum intensity value of the propagated wavefront as in Sec. 3.1.

In Fig. 8, each column shows the amplitude and phase images of the acquired GS CPSFs and the corresponding object reconstruction results from both diffraction and GS correlation methods at specified aberration layer positions. The sampled position of the aberration layer is varied from −5000 to 5000 μm around the desired position. The symbol Δ is the difference between the theoretically desired position and the actual position of the aberration layer. The sign indicates whether the aberration layer moves away from the objective lens (negative) or towards the objective lens (positive). There is the tendency that when the Δ value is larger, the distortion of the phase is smaller and the image is restored better because the imaging property of the system is asymmetric according to the location of the aberration along the z direction. Generally, comparing the GS reconstruction results with the conventional reconstruction results, it is verified that the GS reconstruction yields better results in each region.

3.4 *Discussion*

In the GS reconstruction process, the response of the imaging system with respect to the point source at the object plane can be interpreted as cascading of magnification and a linearly spatial invariant (LSI) function when Eq. (29) is satisfied. Therefore, the point light source located at an arbitrary position relative to the object plane gives a uniform CPSF only with the magnified shift, and the distorted object hologram can be compensated with the GS hologram. When the aberration layer moves from

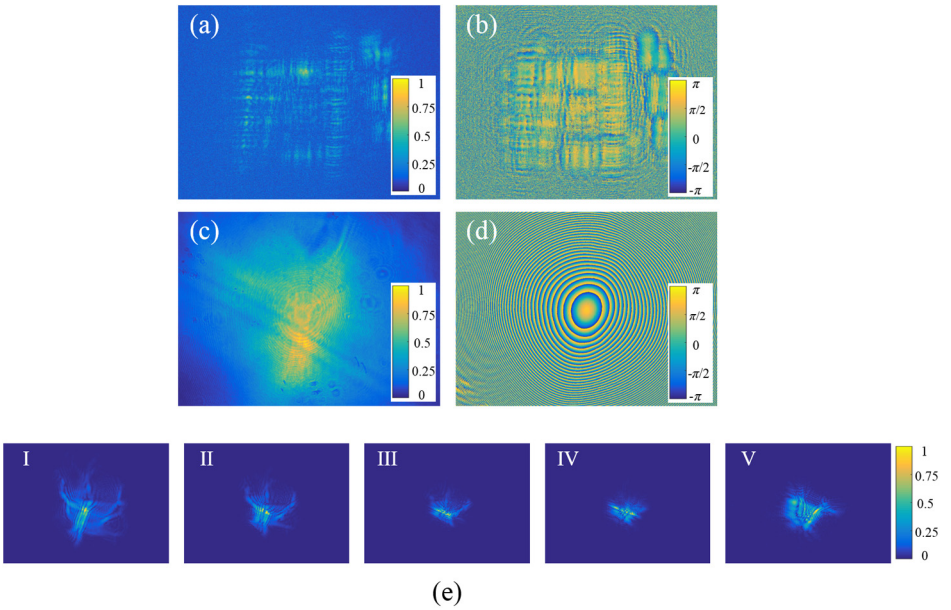

(e)

Fig. 7 (a), (c) amplitude images and (b), (d) phase images of acquired object hologram and GS hologram respectively, and (e) focused image of GS hologram varying the propagation distance near the focusing plane.

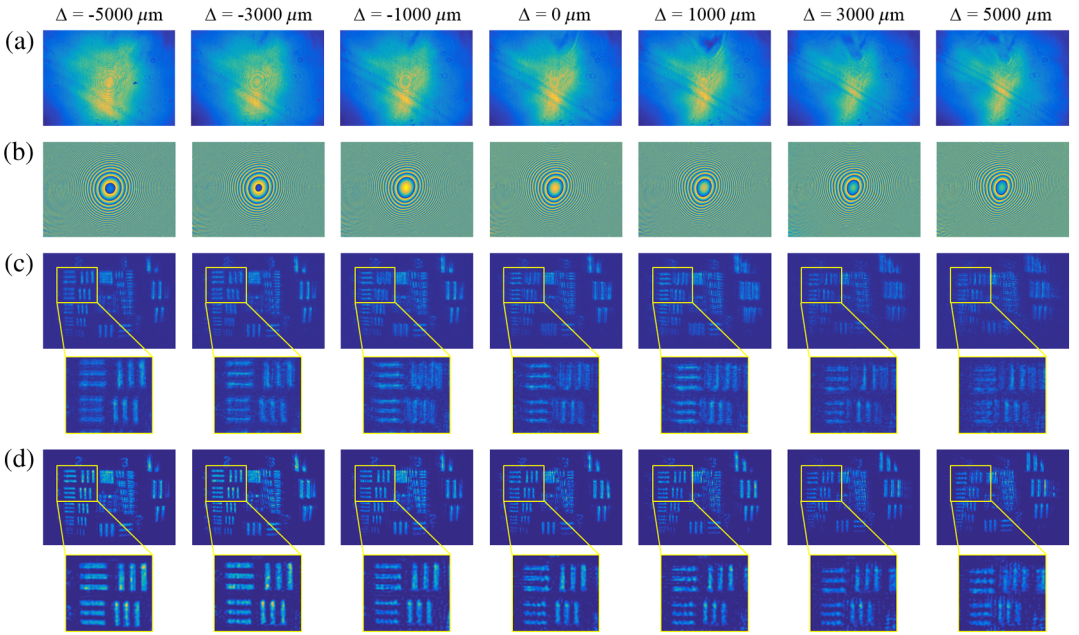

Fig. 8 Acquired GS hologram and numerically reconstructed results of object hologram with angular spectrum method reconstruction and GS reconstruction respectively, according to the position of aberration layer: (a) amplitude image of complex point spread function (CPSF), (b) phase image of CPSF, (c) angular spectrum reconstruction, and (d) GS reconstruction.

the desired position, the LSI characteristic of the system response cannot be guaranteed and the CPSFs of point sources at different positions slowly mismatch each other according to the degree of position error. Even so, as presented in Fig. 8, GS reconstruction shows a better result than the conventional method and we can say that there is clearly a degree of robustness. Therefore, in practical imaging of cells or tissue, in which it could be difficult to define exactly the location or the thickness of the aberrant layer, we expect GS reconstruction is possible to compensate the distorted or blurred image. Also, there is a tendency that the image is compensated better when the aberration layer is closer to the object rather than closer to the objective lens, which implies that the LSI characteristic of the system response changes rather slowly in the case of the former.

In addition, since refocusing is possible in digital holography, the object must not necessarily be at the exact working distance of the objective lens, so the sample object can be simply moved to locate the aberration layer at the desired plane. Therefore, we believe that the presented technique can be the key for imaging fluorescence microscopic objects such as fluorescent stained cells or tissue through an aberrant medium.

4 Conclusion

In this paper, we presented theoretical and experimental demonstration of aberration compensation in HFM using IDHAO. The experimental setup for HFM with IDHAO was designed. Complex holograms of fluorescent microscopic objects and GSs were acquired by three-step phase shifting and image processing. Numerical reconstruction results of the acquired complex holograms were also presented. In the presence of an aberration layer, image reconstruction simulation using a conventional method fails due to an introduced distortion of the wavefront. In contrast, our IDHAO method provides remarkably enhanced reconstruction results. Since it is shown that IDHAO process is robust regarding the location or thickness of the aberration layer, we believe the proposed technique could be applied to the practical situation of cellular imaging. Adaptive optics by SIDH provides new tools for improved cellular fluorescence microscopy through intact tissue layers or other types of aberrant media.

Acknowledgments

Myung K. Kim gratefully acknowledges financial support of Brain Pool Korea by the Ministry of Science, ICT, and Future Planning.

References

1. J. W. Goodman, *Introduction to Fourier Optics*, 3rd ed., Roberts and Company Publishers, Colorado (2004).
2. I. Yamaguchi and T. Zhang, "Phase-shifting digital holography," *Opt. Lett.* **22**(16), 1268–1270 (1997).
3. M. K. Kim, "Principles and techniques of digital holographic microscopy," *SPIE Rev.* **1**(1), 018005 (2010).
4. A. W. Lohmann, "Wavefront reconstruction for incoherent objects," *J. Opt. Soc. Am.* **55**(11), 1555–1556 (1965).
5. G. Cochran, "New method of making Fresnel transforms with incoherent light," *J. Opt. Soc. Am.* **56**(11), 1513–1517 (1966).
6. S.-G. Kim, B. Lee, and E.-S. Kim, "Removal of bias and the conjugate image in incoherent on-axis triangular holography and real-time reconstruction of the complex hologram," *Appl. Opt.* **36**(20), 4784–4791 (1997).
7. J. Rosen and G. Brooker, "Digital spatially incoherent Fresnel holography," *Opt. Lett.* **32**(8), 912–914 (2007).
8. M. K. Kim, "Full color natural light holographic camera," *Opt. Exp.* **21**(8), 9636–9642 (2013).
9. Y. Engelborghs and A. J. W. G. Visser, *Fluorescence Spectroscopy and Microscopy*, Springer Protocols, New York (2014).
10. B. O. Leung and K. C. Chou, "Review of super-resolution fluorescence microscopy for biology," *Appl. Spectrosc.* **65**(9), 967–980 (2011).
11. Y. K. Park et al., "Diffraction phase and fluorescence microscopy," *Opt. Exp.* **14**(18), 8263 (2006).

12. T.-C. Poon, "Scanning holography and two-dimensional image processing by acousto-optic two-pupil synthesis," *J. Opt. Soc. Am.* **2**(4), 521–527 (1985).
13. T.-C. Poon et al., "Three-dimensional microscopy by optical scanning holography," *Opt. Eng.* **34**(5), 1338–1344 (1995).
14. J. Rosen and G. Brooker, "Non-scanning motionless fluorescence three-dimensional holographic microscopy," *Nat. Photonics* **2**(3), 190–195 (2008).
15. H.W. Babcock, "The possibility of compensating astronomical seeing," *PASP* **65**, 229–36 (1953).
16. R. K. Tyson, *Introduction to Adaptive Optics*, The International Society for Optical Engineering, Washington (2000).
17. M. K. Kim, "Adaptive optics by incoherent digital holography," *Opt. Lett.* **37**(13), 2694–2696 (2012).
18. M. K. Kim, "Incoherent digital holographic adaptive optics," *Appl. Opt.* **52**(1), A117–A130 (2013).
19. C. Jang et al., "Holographic fluorescence microscopy with incoherent digital holographic adaptive optics," *Proc. SPIE* **9335**, 933504 (2015).

Changwon Jang is a PhD student at Seoul National University. He received his BS degree in electrical engineering from Seoul National University in 2013. His current research interests include incoherent digital holography, incoherent digital holographic adaptive optics, 3-D imaging, and holographic optical elements. He is the author of more than eight journal papers and seven international conference papers. He is a fellow of the global PhD fellowship program by the National Research Foundation of Korea.

Jonghyun Kim received his BS degree in 2011 in electrical engineering from Seoul National University, Seoul, Republic of Korea. Currently, he is working towards his PhD degree at the School of Electrical Engineering, Seoul National University. His current research interests focus on 3-D display, 3-D imaging, light field microscopy, real-time 3-D visualization system, and stereotest using 3-D display systems. He is the author of more than 10 journal papers and 25 international conference papers.

David C. Clark is a postdoctoral research scholar at the University of South Florida. He received his MS degree in physics at the University of Central Florida in 2006 and his PhD degree in applied physics at the University of South Florida in 2012. He has authored more than 20 journal and conference papers, several by invitation. His current research interests are applications of incoherent digital holography in microscopy, telescopy, and 3-D photographic sensing.

Seungjae Lee is a PhD student at Seoul National University. He received his BS degree in electrical and computer engineering from Seoul National University in 2015. His current research interests include digital holography and 3-D imaging.

Byoungho Lee is a professor in the Department of Electrical Engineering, Seoul National University, South Korea. He received his PhD degree from the Department of Electrical Engineering and Computer Science, University of California, Berkeley, in 1993. He is a fellow of SPIE, OSA, and IEEE, and a member of the Korean Academy of Science and Technology. He served as a director-at-large of OSA and the chair of the Member and Education Services Council of the OSA.

Myung K. Kim is a professor of physics at the University of South Florida and directs the Digital Holography and Microscopy Laboratory. He received his PhD degree from the University of California, Berkeley, in 1986. His current research interests are in the development of novel techniques and applications in digital holography, microscopy, and biomedical imaging. He has more than 200 publications. He is a Fellow of OSA and a Senior Member of SPIE.